Mon. Not. R. Astron. Soc. **271,** 561–572 (1994)

Hysteresis in broad-line regions of active galactic nuclei

Judith J. Perry,[1] Ernst van Groningen[2] and Ignaz Wanders[2]★

[1] *Institute of Astronomy, University of Cambridge, Madingley Road, Cambridge CB3 0HA*
[2] *Astronomiska Observatoriet, Box 515, S-751 20 Uppsala, Sweden*

Accepted 1994 June 2. Received 1994 June 2; in original form 1994 March 17

ABSTRACT

The response of emission-line *luminosities* to changes in the observed continuum in active galaxies is commonly used for reverberation mapping (RM) of the emission-line region. The method assumes regularity in the continuum source and linearity in the line response to the continuum, and that the phase-space distribution of the line-emitting gas is constant in time. The wealth of information contained in the detailed line profiles is under-utilized in current methods of RM. We propose a new method to improve this situation. We define normalized profiles and show how their use enables one to explore details of the emission-line region that have hitherto eluded detection. Furthermore, we investigate the possibility of testing the validity of the assumptions as used in the standard application of RM. We present new methods, the hysteresis test and the Q concept – also based on the line profiles – to test the basic assumptions of RM. The test fails when applied to NGC 4151. We show that there is good evidence either for significantly extended and complex emission-line regions, or for changes in the mass distribution over time-scales of months or more – i.e. on time-scales comparable to the length of typical observing campaigns. We discuss the implication of our results.

Key words: line: profiles – methods: data analysis – galaxies: active – quasars: emission lines.

1 CAN WE MAP THE BROAD-LINE REGION?

The spectra of active galactic nuclei (AGN) are characterized by the presence of broad emission lines whose widths range from approximately 1000 km s^{-1} (FWHM) to more than 10 000 km s^{-1} in some objects. The line spectra contain some of the most detailed quantitative information available about the central regions of AGN, yet the *structure* of the broad-line-emitting region (BLR) is still something of a mystery. Line ratios and intensities are broadly consistent with photoionization by the observed broad-band continuum radiation of dense ($n_e \geq 10^9$ cm^{-3}), optically thick ($N_e > 10^{19}$ cm^{-2}) gas. The mass of gas *directly* involved in line emission can be only a tiny fraction of the total mass of the interstellar medium (ISM) in the galactic nucleus. From line fluxes, the emitting mass can be estimated directly: upper limits range from 1 $M_\odot$ in low-luminosity Seyferts to 100 $M_\odot$ in the most luminous QSOs. The ISM in the region, on the other hand, must contain two to three orders of magnitude more gas (Perry & Dyson 1985). The breadth of the lines means that very high-velocity (almost certainly supersonic) gas is present. This gas must have been accelerated, probably by gravity, radiation pressure or shocks, or some combination of these. Any model of the BLR must account for the physical conditions in the gas, and its geometry and kinematics. Furthermore, the origin of the emitting gas must be both plausible and consistent with the physical and kinematical properties of the nuclear regions of active galaxies.

One of the goals of broad-line observations is to obtain maps of the emission-line region of sufficiently good quality to enable choices to be made between theoretical models. Since the emission-line region is unresolvable by present observational techniques, reverberation mapping (RM) has become the favoured tool for examination of the physical structure of the region. RM is based on analysis of the time response of the lines to the continuum variations.

Variations in the broad-emission-line *strengths*, in AGN with continuum variability, are a characteristic feature of AGN spectra (Andrillat & Souffrin 1968; Cherepashchuk & Lyutyi 1973). This behaviour, most naturally, has been explained as the response of the emitting gas to the changes in the exciting continuum radiation which it is reprocessing. The study of this variability – in principle – should allow observers to 'map' the BLR (Bahcall, Kozlovsky & Salpeter 1972; Blandford & McKee 1982, henceforth BMK; Gaskell & Sparke 1986). Because of finite light traveltimes, the

★ Present address: Department of Astronomy, The Ohio State University, 174 West 18th Avenue, Columbus, Ohio 43210, USA.

observed response of the emitting gas should be smeared out and delayed with respect to the continuum, and should reveal the spatial distribution of the gas.

Reverberation mapping (see e.g. Peterson 1988, 1993 for recent reviews), as the study of the delay (lag) has become known, originally arose out of the standard model for the emission-line region – that of small, long-lived, dense clouds moving through the region with a regular and systematic velocity structure (for a review of BLR models, see Perry 1993). This standard model, however, no longer appears reconcilable with observations, and numerous other theoretical models are currently under study. The different geometrical and velocity distributions predicted by these models should be distinguished by different line profiles, and by different reverberation maps. Furthermore, the evolution of the spatial and velocity distributions of line-emitting material – which are also different in the different dynamical models – should likewise be distinguishable in the temporal behaviour of the line *profiles*.

However, although – in principle – reverberation maps give us information about the structure of the BLR, one has to make numerous assumptions for these methods to work (e.g. Penston 1991; Krolik 1992). These include the assumptions that the continuum is emitted by a point source, that the observed continuum is indicative of the ionizing continuum, that the lines respond in a linear manner to changes in the continuum, and that the distribution of line-emitting material is constant in time. Both RM and line profile modelling currently are used to test models for the kinematics and geometry of the BLR, but their use has not yet been able to constrain parameter space significantly.

On the basis of the first analyses of AGN spectra, which showed remarkably short lags, it was concluded that the emitting gas is significantly closer to the continuum source than the characteristic distances determined from photoionization calculations. *If* the emitting gas exists in a shell, thin in comparison to its distance from the central source and steady in time, then the measured lag is a direct measure of the distance of the gas from the ionizing continuum. However, as discussed by Penston (1991), RM is far more complicated than the usual simple assumptions would imply. When the emission-line region is extended, the lag is heavily biased towards the *inner boundary* of the region (Gaskell & Sparke 1986; Robinson & Pérez 1990; Pérez, Robinson & de la Fuente 1992). The centroid of the cross-correlation function corresponds – in principle – to the *luminosity-weighted radius* (Robinson & Pérez 1990). The detailed simulations of Pérez et al. (1992) illustrate some of the dangers in interpreting variability data – they show that even the ideal of measuring the inner radius and luminosity-weighted radius may not be achieved in practice, since the results are very dependent on sampling techniques. Our findings, in this paper, support the possibility that the BLR is much larger than its luminosity-weighted radius suggests.

A further complication arises because, despite the complexities in the observed line spectra, one systematic trend *has* emerged in the data: a separation of the low- and high-ionization line-emitting regions (the LIL and HIL respectively). The systematic blueshift of the HIL with respect to the LIL (Gaskell 1982; Espey et al. 1989), combined with the differences in the conditions required for the photoionization equilibrium in the two regions (Wills, Netzer & Wills 1985; Collin-Souffrin et al. 1986) has led to the conclusion that, minimally, two physically distinct components are necessary to model the BLR successfully. Furthermore, these two components are excited by different parts of the ionizing continuum. Thus observed reverberation maps may well be the superposition of reverberation in *at least* two components. This complexity in the structure of the BLR, deduced from models of the 'steady-state' line spectra, is supported strongly by recent monitoring campaigns which find that the observed lags for the emission lines differ from line to line (Maoz et al. 1994).

Furthermore, RM *assumes* a stable cloud population. If the emitting gas condensations are ephemeral, this introduces additional complications into the analysis; yet there are good hydrodynamic reasons for supposing that temporal changes in the physical structure of the region – or mass redistribution (MRD) – may be common, since this can be expected on hydrodynamical grounds (Perry & Dyson 1985; Perry 1993). In particular, there are two primary forms of MRD: that due to large-scale motions, and that due to cloud creation and destruction. Thus, although line variability studies do place constraints on models, it is not yet clear exactly what the physical interpretation of the observations is.

The information contained in the profiles, particularly their temporal properties, has not yet been used fully. The observations clearly reveal not only that the line intensities change, but also that their profiles vary. To date, no clear systematic trends have emerged in the behaviour of the line profiles. Given the complexity of the nuclear region, and the expected diversity in, for example, the angular momentum of the system and the possibility of both winds and accretion flows, it would seem logical to conclude that there can be a wide diversity in the detailed motions and distribution of the line-emitting gas.

In this paper we propose new methods to utilize better the detailed information contained in the line profiles. We re-express the standard transfer function of reverberation mapping, dividing it into a dominant, steady-state part and a 'deviation' term; we then define normalized profiles which can be used to measure the 'deviation' term. The use of these normalized profiles enables one to explore details of the emission-line region that have heretofore eluded detection. We then investigate the possibility of testing the validity of some of the basic assumptions of reverberation mapping. In particular, both in the use of the normalized profiles and in our tests of the basic assumptions of RM, we concentrate on whether direct observational evidence exists for extended broad-line regions with complicated velocity structures, or for changes in the matter distribution in the region of time-scales comparable to the variability time-scale.

In a recent paper, Ulrich et al. (1991) found evidence for MRD in the BLR of NGC 4151, using the large *IUE* data base on this galaxy. Their conclusion was based on changes in the asymmetry of the C IV λ1550 line, which they suggest is not only the result of ionizing continuum variations. In this paper we examine their conclusion by using the more careful approach outlined in Section 5.3.

In Section 2 we review briefly the principles of the standard methods of RM as currently used, and extend these in Section 3 by introducing the normalized profiles and the 'Q' function and applying these concepts to the Balmer lines

of NGC 3516. In Section 4 we discuss the difficulties introduced if the standard assumptions about the structure and dynamics of the BLR are not valid. In Section 5 we outline new approaches toward solving these problems and apply these new approaches to NGC 4151. We summarize and discuss our results in Section 6.

2 REVERBERATION MAPPING REVISITED

The emission-line intensities and profiles depend on (i) the temporal history of the ionizing continuum preceding the observation over a time-span corresponding to twice the light crossing time of the BLR, (ii) the distribution in phase space of the line-emitting material, (iii) line transfer in the region, and (iv) the angular distribution of the ionizing radiation. Here we briefly review the concept of RM and summarize the definitions of several quantities which we will need later. We follow the notation adopted by BMK.

Because of light traveltime effects, the emission-line flux variations lag the ionizing continuum variations. Mathematically, this is commonly written as a convolution integral:

$$L_\ell(v, t)=\int_{-\infty}^{\infty} \mathrm{d}\tau\, L_c(t-\tau)\Psi_\ell(v, \tau). \tag{1}$$

Here, $L_\ell(v, t)$ is the flux observed in a particular emission line ℓ at time t at the projected Doppler-shifted velocity v, and $L_c(t)$ is the ionizing continuum flux. $\Psi_\ell(v, \tau)$ is referred to as the two-dimensional transfer function (TF) of the BLR, where τ is the delay time. The geometry, kinematics and physical conditions of the BLR gas and the continuum source are all contained in $\Psi_\ell(v, \tau)$. Causality of the system implies that $\Psi_\ell(v, \tau)=0$ for $\tau<0$.

In the standard RM picture, the following assumptions are made:

(1) (ii)–(iv) above are time-independent;
(2) the central ionizing source is small compared to the emission-line region;
(3) the recombination time is short compared to the characteristic variability time-scale of the continuum;
(4) the ionizing continuum exciting the lines is directly proportional to the observed continuum flux; and
(5) the line fluxes have a linear, time-independent dependence on the exciting continuum, which then implies that $\Psi_\ell(v, \tau)\geq 0$ for $\tau\geq 0$.

So far, no large spectral-monitoring campaign has conclusively shown *profile* variations that are caused by the reverberation effects in the BLR.

2.1 The steady-state line profile $\Phi_\ell(v)$

If the ionizing continuum is constant in time, $L_c(t)\equiv L_0$, then the line profile is also time-independent and defines the steady-state profile, $\Phi_\ell(v)$:

$$L_\ell(v)=L_0\int \mathrm{d}\tau\, \Psi_\ell(v, \tau)\equiv L_0\Phi_\ell(v). \tag{2}$$

Furthermore,

$$L_\ell=L_0\int \mathrm{d}v\, \Phi_\ell(v)\equiv L_0 W_\ell. \tag{3}$$

$\Phi_\ell(v)$ is the function predicted by line profile calculations based on BLR models, and W_ℓ is a nominal equivalent width. Both $\Phi_\ell(v)$ and W_ℓ are defined here in arbitrary flux and length units, since the absolute flux levels depend both on the choice of reference frequency for L_0 and on the full spectral shape of $L_c(t)$; in theoretical line profile calculations, it is assumed that the spectral shape of the continuum is known and that the total continuum luminosity can be scaled to any frequency. If the continuum is scaled to the monochromatic luminosity at the line centre, then W_ℓ is the usual equivalent width. Independent of this arbitrary scaling, however, the ratio W_1/W_2 is the line ratio between the lines 1 and 2 predicted by BLR models.

It is important to note that $\Phi_\ell(v)$ and W_1/W_2 can only be compared directly with profiles and line ratios observed at single epochs if reverberation effects are negligible. For a variable source, an estimated $\Phi_\ell(v)$ can be obtained by taking the time averages of the emission-line profiles and the continuum:

$$\langle L_\ell(v, t)\rangle=\langle L_c(t)\rangle\Phi_\ell(v). \tag{4}$$

This is, strictly speaking, only valid for an infinite continuous, stationary time series; in Section 5.1.2, however, we discuss alternative ways to determine $\Phi_\ell(v)$ for variable sources.

2.2 The one-dimensional transfer function $\Psi_\ell(\tau)$

At any time t, the integrated intensity in an emission line can be expressed as

$$\begin{aligned} L_\ell(t)&=\int \mathrm{d}v \int \mathrm{d}\tau\, L_c(t-\tau)\Psi_\ell(v, \tau) \\ &=\int \mathrm{d}\tau\, L_c(t-\tau)\Psi_\ell(\tau); \end{aligned} \tag{5}$$

here $\Psi_\ell(\tau)$ is the one-dimensional transfer function. Reverberation mapping experiments based on total line intensities recover $\Psi_\ell(\tau)$, rather than the full two-dimensional transfer function (Peterson 1993).

2.3 Observational derivation of the transfer function

The TF can be reconstructed by inverting equation (1), using the convolution theorem and the usual definition of the Fourier transforms of L_ℓ and L_c, i.e.

$$\tilde{L}_\ell(v, \omega)=\int_{-\infty}^{\infty} \mathrm{d}t\, \mathrm{e}^{\mathrm{i}\omega t} L_\ell(v, t). \tag{6}$$

It is then found that (BMK)

$$\Psi_\ell(v, \tau)=\frac{1}{2\pi}\int_{-\infty}^{\infty} \mathrm{d}\omega\, \mathrm{e}^{-\mathrm{i}\omega\tau}\frac{\tilde{L}_\ell(v, \omega)}{\tilde{L}_c(\omega)}. \tag{7}$$

Thus – in principle – observations of L_ℓ and L_c can be used to find the TF directly. Fourier transform methods, however, are very sensitive to the noise and irregular sampling which characterize current observations, and cannot be used for those time-scales on which the continuum

does not vary. In addition, to use these methods, long series of observations are required. The maximum entropy method is an alternative method of deconvolving equation (1) to derive the TF from the data which circumvent some of these difficulties (Skilling & Bryan 1984; Horne, Welsh & Peterson 1991).

2.4 From the transfer function to BLR distributions

The determination of the TF is not in itself a determination of the actual physical distribution of the BLR gas. The goal of RM of the BLR is ultimately to determine the distribution of the line-emitting mass density, $\rho(\boldsymbol{r}, t)$, and the phase-space density, $f(\boldsymbol{r}, \boldsymbol{w}, t)$, of the line-emitting 'clouds' as functions of position in the BLR, $\boldsymbol{r}$, velocity of the broad-line-emitting gas, $\boldsymbol{w}$, and time, t.

In standard RM, both ρ and f are assumed to be independent of time. The density and temperature of the BLR gas are subsumed in the reprocessing coefficient, $\varepsilon_\ell(\boldsymbol{r})$, according to

$$j_\ell(\boldsymbol{r}, t)=\frac{\varepsilon_\ell(\boldsymbol{r})L_c(t-r/c)}{4\pi r^2}, \tag{8}$$

where $j_\ell(\boldsymbol{r}, t)$ is the volume emissivity in erg cm^{-3} s^{-1} in a given line. The emissivity depends on (i) where the matter is, i.e. the BLR cloud density ρ, (ii) the ionizing radiation flux $L_{\rm ion}(t-r/c)$, and (iii) the response of the medium to the ionizing radiation, $L_{\rm line}=\mathscr{F}[L_{\rm ion}(t-r/c)]$. Clearly, the last two points are coupled with each other.

The assumption that the line emission responds linearly to continuum variations, i.e. that $\mathscr{F}$ is linear or that $\varepsilon_\ell(\boldsymbol{r})$ is independent of the incident continuum flux, is built into the form used here for $j_\ell(\boldsymbol{r}, t)$ (equation 8). Furthermore, since the matter distribution, expressed through $\varepsilon_\ell(\boldsymbol{r})$, is taken as time-invariant, the time dependence of $j_\ell(\boldsymbol{r}, t)$ is due only to the time dependence of L_c. As we discuss later (see Section 4.2), however, the line response may well be non-linear, and the matter distribution time-dependent. *Equation (8) is essential to the definition of the TF in equation (1), and to the extraction of physical quantities from the TF.*

Under the assumption that there is no absorption or scattering of the emitted line radiation, the observed line profile can be written as a function of the emissivity and the velocity distribution $f(\boldsymbol{r}, \boldsymbol{w})$ (BMK):

$$L_\ell(v, t)=\int \mathrm{d}\boldsymbol{r}\,\mathrm{d}\boldsymbol{w}\,\mathrm{d}t'\,j_\ell(\boldsymbol{r}, t')f(\boldsymbol{r}, \boldsymbol{w})\,\delta(v-\boldsymbol{n}\cdot\boldsymbol{w}) \times \delta(t'-t+\boldsymbol{n}\cdot\boldsymbol{r}/c), \tag{9}$$

where $\boldsymbol{n}$ is a unit vector pointing from the distant observer to the source.

The line-of-sight velocity distribution function $g(\boldsymbol{r}, v)$ is defined as

$$g(\boldsymbol{r}, v)=\int \mathrm{d}\boldsymbol{w}\,f(\boldsymbol{r}, \boldsymbol{w})\,\delta(v-\boldsymbol{n}\cdot\boldsymbol{w}). \tag{10}$$

It is convenient to scale f such that $\int f\,\mathrm{d}\boldsymbol{w}=1$, and hence $\int g\,\mathrm{d}v=1$ as well. By inserting relations (8) and (10) into (9) and comparing with (1), one finds

$$\Psi_\ell(v, \tau)=\int \mathrm{d}\boldsymbol{r}\,\frac{\varepsilon_\ell(\boldsymbol{r})g(\boldsymbol{r}, v)}{4\pi r^2}\,\delta[\tau-(r+\boldsymbol{n}\cdot\boldsymbol{r})/c]. \tag{11}$$

The sport is to invert equation (11) to find the product $\varepsilon_\ell(\boldsymbol{r})g(\boldsymbol{r}, v)$. This is usually impossible to do analytically, but it can be done for special cases by making specific assumptions about the functional forms of $\varepsilon_\ell(\boldsymbol{r})$ and $g(\boldsymbol{r}, v)$. BMK give several examples of special BLR geometries and kinematics which allow such inversion. The hope of many astronomers during recent years has been to observe L_ℓ and L_c well enough and for long enough to be able to compare observationally determined TFs with theoretically derived ones, in order to infer the geometry and kinematics of the BLR. As we discuss in the following section, there may be important problems thwarting this hope.

3 NORMALIZED PROFILES AND THE *Q*-CONCEPT

Observationally it is relatively straightforward to determine separately the one-dimensional TF, $\Psi_\ell(\tau)$, and the steady-state line profile, $\Phi_\ell(v)$. On the other hand, the determination of $\Psi_\ell(v, \tau)$ has proven to be extremely difficult (Peterson 1993).

Results available to date (Maoz et al. 1991; Clavel 1991; Wanders & Horne 1994) appear to indicate that the full TF is the product of $\Psi_\ell(\tau)$ and $\Phi_\ell(v)$ – which would be the case for a BLR with a spatially homogeneous, random velocity field. In this case the profiles should be symmetrical. However, time-dependent profile asymmetries *are* observed. These could, for example, be easily explained if systematic velocity fields were superposed upon dominant random motions. Alternatively, these changes may reflect real time variability in the BLR.

It is important for our understanding of the region to attempt to determine the significance and source of these variations. The details of the observed velocity structure and its evolution are enhanced by a process of normalization of the emission-line profiles, which removes the dominant effects of line intensity changes. We outline the method, and its relationship to the TF, below. We then apply this method to the Seyfert 1 galaxy NGC 3516, which has been the subject of extensive RM campaigns.

3.1 The *Q*-concept

We separate the TF into a 'steady-state total-flux' part and a 'deviation' part following standard first-order Taylor series expansion methods under the usual assumptions of analyticity:

$$\Psi_\ell(v, \tau)=\frac{\Phi_\ell(v)\Psi_\ell(\tau)}{W_\ell}+Q_\ell(v, \tau). \tag{12}$$

The importance of splitting the TF in this fashion becomes clear when we examine the properties of the function $Q_\ell(v, \tau)$. We integrate equation (12) over v and τ individually to obtain

$$\int \mathrm{d}\tau\,Q_\ell(v, \tau)=\int \mathrm{d}v\,Q_\ell(v, \tau)\equiv 0. \tag{13}$$

$Q_\ell(v, \tau)$ can be related to observed emission-line profiles through the following normalization procedure. Define the total integrated line flux, $L_\ell(t) = \int \mathrm{d}v\, L_\ell(v, t)$, and the normalized emission-line profile

$$L_n(v, t) = \frac{L_\ell(v, t)}{L_\ell(t)} = \frac{1}{L_\ell(t)} \int \mathrm{d}\tau\, \Psi_\ell(v, \tau) L_c(t - \tau). \tag{14}$$

Insertion of equation (12) into (14), using equation (13), and rearrangement of terms yield

$$L_\ell(t) \left[L_n(v, t) - \frac{\Phi_\ell(v)}{W_\ell} \right] \equiv L_q(v, t) = \int \mathrm{d}\tau\, Q_\ell(v, \tau) L_c(t - \tau). \tag{15}$$

The left-hand side of equation (15) contains only observable quantities; its calculation does not increase the absolute noise level significantly because $\Phi_\ell(v)$, W_ℓ and $L_\ell(t)$ are known to much higher accuracy than is $L_\ell(v, t)$.

Equation (15) expresses an inversion problem similar to that stated in equation (1). The primary difference from the standard RM inversion problem is that $Q_\ell(v, \tau)$ is extremely sensitive to all the reverberation effects in velocity space (i.e. those due to structural details or to short-time-scale temporal changes in the region), whereas $\Psi_\ell(v, \tau)$ is mainly sensitive to the total-flux reverberation effects through the dominant first term in equation (12).

In the following section, we examine a specific example in more detail.

3.2 NGC 3516

This Seyfert 1 galaxy was observed during the LAG monitoring campaign at the La Palma Observatory during the first five months of 1990. A full description of the observations is presented by Wanders et al. (1993). A total of 22 Hα spectra and 21 Hβ spectra were obtained with a typical signal-to-noise ratio in the continuum of ~ 100 for the Hα spectra and ~ 50 for the Hβ spectra. The resolution of the spectra is 3 Å. The continuum flux level was deduced from the Hβ spectra after correction for starlight from the bulge of NGC 3516. The high quality of these optical spectra allows detailed analysis of the line profile variations.

To obtain the broad-line profiles, a continuum was subtracted from all Hα and Hβ spectra, and the lines cleaned of their narrow-line contributions, using the [O III] λ5007 profile as a template. Then, for each epoch, these pure Hα and Hβ broad-line profiles were normalized, so that the total integrated area under the line – within the wavelength region corresponding to -5500 to $+5500$ km s^{-1} – is unity. The same normalization was then done for the *mean* of all the line profiles. This *normalized mean profile*, equal to $\Phi_\ell(v)/W_\ell$ (see Section 3.1; Wanders 1994), was then subtracted from the individual normalized profiles and this result was multiplied by the total flux in the emission line, following equation (15). This resulted in two sets of 'residual-shape spectra', one for Hα and one for Hβ, which are presented in Fig. 1

From Fig. 1 it is immediately clear that the shape variations are smooth in time and similar for Hα and Hβ, although differences between Hα and Hβ do seem to exist, especially during the first half of the campaign. Note that the normalization of the Hβ fluxes is slightly influenced by the absorption dip in the blue wing of Hβ at ~ -1200 km s^{-1} (cf. Wanders et al. 1993) and the complexity of the spectrum in its far red wing due to residuals of [O III] and possibly Fe lines. The dominant shape variations occur in the blue wing and in the cores of the lines, whereas the shape of the red wing is nearly constant over the time spanned by these spectra (cf. Wanders & Horne 1994). A 'double-valley' shape variation is visible in both Hα and Hβ around 1990 March 31. Significant shape variations take place on a time-scale of ~ 2 weeks.

We have measured 'fluxes' in these 'residual-shape spectra' in three wavelength intervals: the blue wing ($-5000 < v < -1700$ km s^{-1}), the line core ($-1700 < v < +1700$ km s^{-1}) and the red wing ($+1700 < v < +5000$ km s^{-1}). In this way, three light curves have been constructed, representing the relative importance of the emissivity in a particular part of the emission line at a given epoch relative to the mean. These relative-emissivity time series are presented in Fig. 2, together with the measured continuum and total line flux light curves from Wanders et al. (1993). It can be seen that both the Hα and the Hβ line *shapes* behave almost identically, and that both are seemingly independent of the continuum and total line flux light curves.

In Fig. 3 we present the autocorrelation functions (ACFs) of the flux light curves and the shape time series. The ACFs of the shape time series are very broad and flat, suggesting that shape variations occur on much longer time-scales than do flux variations. The cross-correlation function (CCF) of the shape 'core' time series in response to the continuum flux is presented in the upper right panel of Fig. 3. The peak of the CCF lies at 20 ± 3 d, which is significantly larger than the 14 ± 2 d found for the total Hα flux response by Wanders et al. (1993). The fact that the CCF can be narrower than the ACF for the shape time series is due to the time series containing negative values ('responses': Sparke 1993). The half-width at half-maximum (HWHM) for the flux light curves ACF is 9 d for the continuum, 13 d for the Hα line and 14 d for the Hβ line. The cores, blue wings and red wings of the lines yield the same HWHM (to within the errors of ~ 2 d) for their ACFs as do the total line fluxes. However, the shape time series yield HWHM of ~ 35 d for both the blue wing and the core of the lines. (The red wing does not give a significant result because its shape is nearly constant in time and its time series is dominated by noise: cf. Fig. 2.)

Thus the profile variations occur on a much longer time-scale than do the total flux variations. If the changes are caused by reverberation, this would mean that $Q_\ell(v, \tau)$ has significant signal at large lags, and that therefore $\Psi_\ell(v, \tau)$ also must have significant structure at these large lags. From this we conclude that the BLR is probably much larger than the total-flux TF indicates. This result is in accordance with the simulations done by Robinson & Pérez (1990). Our time series is still too short to determine unambiguously the TF of NGC 3516, however, and we cannot choose between the alternate physical explanations for $Q_\ell(v, \tau)$ – that the BLR is large and complex, and that mass redistribution is occurring on time-scales of roughly one month. We now turn to methods of addressing these questions.

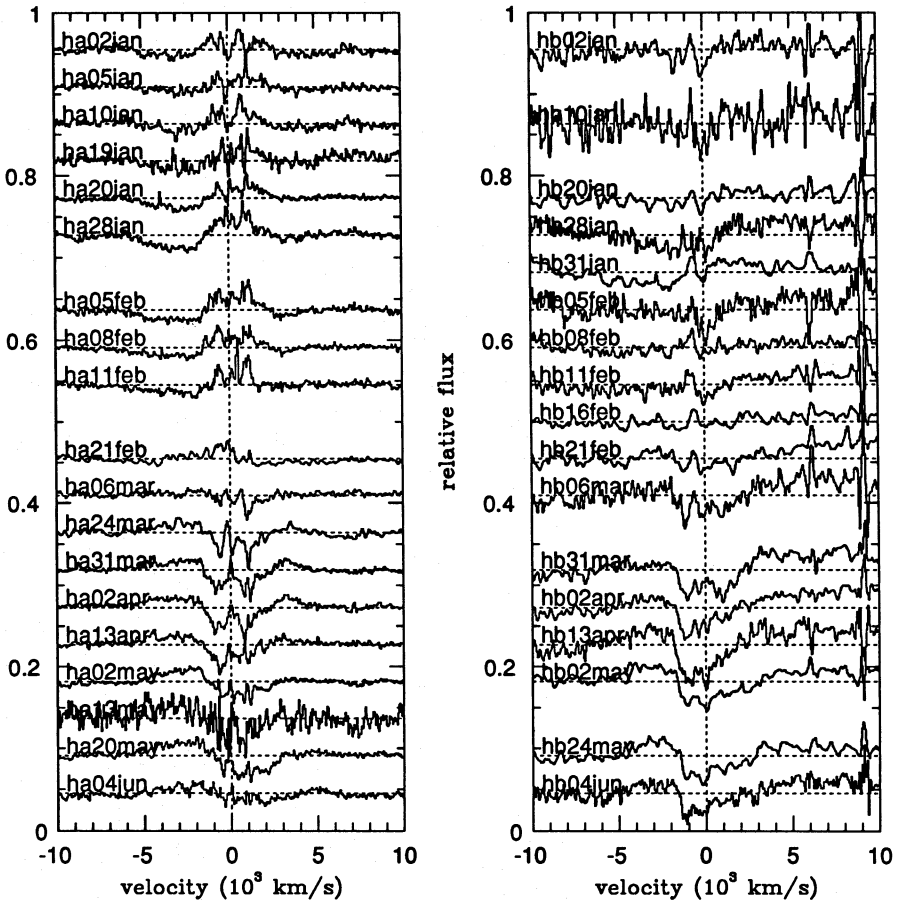

Figure 1. The residual-shape spectra $L_q(v, t)$ of both Hα (left) and Hβ (right) of NGC 3516, as defined in equation (15).

4 WHY THERE ARE PROBLEMS IN MAPPING THE BLR

Apart from line profile changes due to reverberation effects, genuine changes in line profiles can be caused by a number of factors, some of which imply that the standard reverberation picture is in deep trouble. There are three main contributing factors: mass redistribution in the BLR; non-linearity in the line response; and our poor understanding of the properties of the continuum source. We now discuss these in turn.

4.1 Mass redistribution in the BLR

The assumption that the physical structure of the BLR – its mass distribution and velocity structure – is time-independent underlies standard RM. Yet large variations in the continuum may have important dynamical consequences for the gas in the BLR, in addition to their effects on the ionization structure. Furthermore, so long as the physical origins of the observed continuum variations are not understood, it is unclear whether they are caused, at least in part, by physical changes in the gas flows supplying the continuum source.

Changes in the structure of the line-emitting gas, or mass redistribution (MRD), can arise both because of large-scale motions and because of local changes to the density or velocity fields. Large-scale motions, for example random orbits of an inhomogeneous cloud population, have time-scales of typically $\sim R_{\rm BLR}/|w| \approx (c/|w|)\,\tau_{\rm LT}$, where $\tau_{\rm LT}$ is the light traveltime across the BLR. Because $c/|w| \gg 1$, these effects are expected to be negligible over the (relatively) short times of most monitoring campaigns, which typically last only a few $\tau_{\rm LT}$. However, if the clouds – or, more properly, the cold gas condensations – are not dynamically stable structures, they can change their internal structure on time-scales of the order of their internal sound crossing time, $\tau_{\rm sc} \approx r_{\rm cloud}/w_{\rm sound} \approx N_{\rm e}/n_{\rm e}\,w_{\rm sound} \leq 50$ d – similar to the length of most monitoring campaigns. Here, $N_{\rm e}$ and $n_{\rm e}$ are the cloud column and volume number densities, respectively.

Cloud formation and destruction also occur on similar time-scales, when unstable line cooling sets in behind radiative shocks (Perry & Dyson 1985). In such situations, the overall structure of the region changes on the much longer time-scales for radiative cooling of the shocks themselves, which vary from years in the models of Terlevich and his collaborators (Terlevich et al. 1992), to tens of years in the Perry–Dyson models. However, changes in the structure of the post-shock cold gas condensations can occur on the smaller time-scales of $\sim \tau_{\rm sc}$. Since the goal of RM is to delineate the structure of the BLR well enough to discrimin-

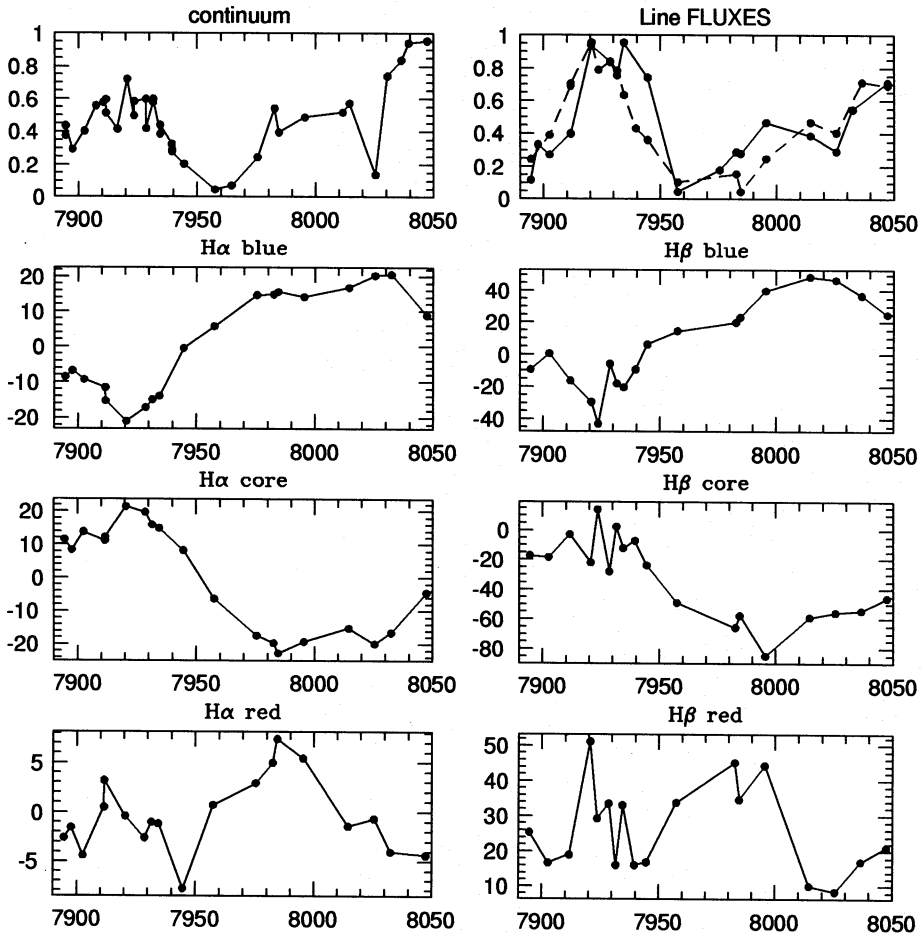

Figure 2. The flux light curves of the optical continuum, the Hα line (solid) and the Hβ line (dashed) of NGC 3516 (Wanders et al. 1993), as well as the three 'shape' time series for Hα and Hβ. See the text for the details.

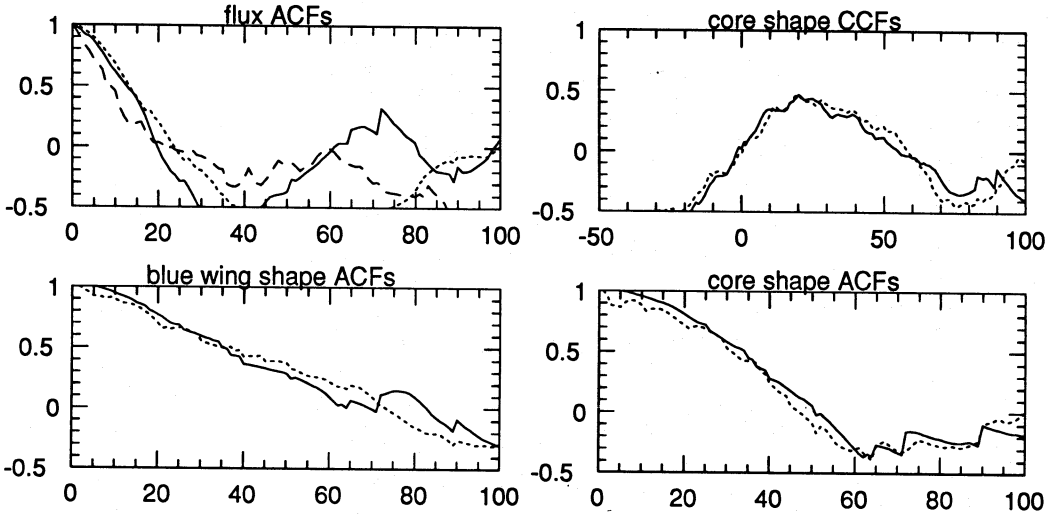

Figure 3. The ACFs of the flux light curves and the shape time series, as well as the CCFs of the shape cores in response to the continuum flux. The solid line depicts Hα, the short-dashed line Hβ, and the long-dashed line the continuum flux.

ate between dynamical models, sensitivity to possible MRD effects is important.

MRD implies that $\varepsilon_\ell(\boldsymbol{r})$ and $f(\boldsymbol{r}, \boldsymbol{w})$ are both functions of time and, therefore, so also is $g(\boldsymbol{r}, v)$. In equations (5) to (8) we then have to replace ε_ℓ, f and g by their general forms $\varepsilon_\ell(\boldsymbol{r}, t)$, $f(\boldsymbol{r}, \boldsymbol{w}, t)$ and $g(\boldsymbol{r}, v, t)$. Although the TF is still well defined through equation (8), it is now time-dependent: it is given by $\Psi(v, \tau, t)$ and can no longer be found, observation-

ally, through equation (4). It must be found via other methods, e.g. maximum entropy methods (Wanders & Horne 1994). In the case that MRD is present, however, the TF may not be the most suitable tool for analysis of the structure of the BLR, since MRD implies that the BLR is inhomogeneous (cf. Wanders 1994). In the following sections, we present several tests of the validity of RM; some of these can be extended to provide tools which can be used to measure the evolution of the TF, in the case that MRD is present.

4.2 Non-linear line response

The assumption that the lines respond linearly to continuum variations is also incorporated into standard RM. Yet, for example, opacity effects in optically thick columns introduce non-linearity.

Non-linearity implies that $\varepsilon_\ell(\boldsymbol{r})$ is dependent on the incident continuum flux, and hence

$$j_\ell(\boldsymbol{r}, t) = \varepsilon_\ell[\boldsymbol{r}, L_c(t' - r/c)/4\pi r^2]\frac{L_c(t' - r/c)}{4\pi r^2}. \quad (16)$$

It is clear that now any transfer function also will depend on L_c, and that it is no longer possible to derive a simple analogue for equation (8). It is possible, however, to write the analogue of equation (1) as

$$L_\ell(v, t) = \int_{-\infty}^{\infty} \mathrm{d}t' L_c(t')\Upsilon(v, t - t', L_c), \quad (17)$$

where $\Upsilon(v, t)$ is the 'non-linear' TF. Maximum entropy methods and model fitting have been used to derive $\Upsilon(v, t, L_c)$ directly in particular cases (Maoz 1992; Sparke 1993; Goad, O'Brien & Gondhalekar 1993). The hysteresis test that we discuss in Section 5.1.1 is unaffected by non-linear line response, and can be used to disentangle non-linearity from MRD and continuum source effects.

4.3 Properties of the continuum source

4.3.1 *Time-varying anisotropy and spectral index*

The assumption that the observed optical or UV continuum is a good indicator of the ionizing continuum is fundamental to RM. There are several situations for which this may not be the case.

If the continuum is emitted anisotropically, but its angular distribution is not constant in time, then the flux reaching the BLR is not related directly to that observed. This is a fundamental problem which is difficult to constrain observationally.

If the continuum spectral shape is time-variable, then a simple proportionality between the observed and ionizing continua does not necessarily exist. This problem may not be too serious, since recent monitoring of X-ray and optical/UV continua has shown that there exists a nearly linear correlation between the UV flux and the X-ray flux, at least in some objects (Ulrich et al. 1991; Clavel et al. 1992). Conflicting evidence exists, however, which indicates non-correlated variations in e.g. NGC 5548 (Yaqoob et al. 1993). More multi-wavelength monitoring campaigns will be needed to establish the generality of these results. However, the fact that – to first order – the lines do vary in response to variations in the *observed* continuum means that spectral variations cannot be totally uncorrelated. In light of the sparseness of the data, and the inconclusiveness of the existing results, we conclude that this question remains open.

4.3.2 *Non-compact continuum source*

A central, compact continuum source is also one of the basic assumptions of RM. If the exciting continuum comes from an extended source, or from multiple sources, it is not possible to incorporate this in a simple manner into the RM, since again the analogue of equation (8) is not defined. In this case, L_c depends not only on time but also on position $\boldsymbol{r}$. Examples of extended continuum sources are, amongst others, the pure starburst model of AGN (Terlevich et al. 1992) where the BLR and continuum sources are spatially coincident, and models where the BLR is illuminated both by a compact central source and by light scattered on a medium of non-negligible size, e.g. in X-ray reflection models (Collin-Souffrin 1987; Collin-Souffrin et al. 1988). X-ray observations of NGC 5548 indicate that reprocessing on a scale of 10–20 light-days may occur (Pounds, Nandra & Stewart 1992).

5 TESTING THE BASIC ASSUMPTIONS OF RM

One of the aims of this paper is to develop direct observational tests of the validity of the assumptions of standard RM, and to begin to disentangle the problems listed in the previous section. To this end, we develop three observational tests based on line profiles in combination with specific properties of the light curves, such as repetition, scaling or shifts. These tests are very powerful; in practice, however, there is a snag. The irregularity in the observed continua means that we require great good fortune or extensive monitoring campaigns to find useful episodes in the continuum variation. We first develop the formalism of the three null tests, and discuss what conclusions can be drawn when these tests are violated (Section 5.1); we then apply these tests to NGC 4151 (Section 5.2). We conclude with a proposal (Section 5.3) for the use of these tests to derive evolutionary information about the TF.

5.1 Null tests of the validity of standard RM assumptions

Our null tests are all formulated in terms of the continuum look-back light curve, $\mathscr{L}_1(\tau)$, which is defined such that, at time t_1, $\mathscr{L}_1(\tau) \equiv L_c(t_1 - \tau)$. Then

$$L_\ell(v, t) = \int \mathrm{d}\tau \mathscr{L}(\tau)\Psi_\ell(v, \tau). \quad (18)$$

5.1.1 *Hysteresis of line profiles*

An important truism of standard reverberation mapping is that *line profiles should be identical at two different instants if the ionizing light curves preceding these instants were identical over times corresponding to twice the light traveltime across the line-emitting region:* $2\tau_{LT} = 2c \times R_{BLR}$.

Thus the strongest test for the validity of the standard assumptions of RM is clearly that a subtraction of line profiles at two instants with identical $\mathscr{L}(\tau)$ should yield a

zero residual, i.e. $L_\ell(v, t_2) - L_\ell(v, t_1) = 0$ if $\mathscr{L}_2(\tau) = \mathscr{L}_1(\tau)$ for all $0 \le \tau \le 2\tau_{\rm LT}$, because $\Psi(v, \tau > 2\tau_{\rm LT}) = 0$. [If the line response is linear, this can be generalized to three epochs with look-back light curves which satisfy $\mathscr{L}_3(\tau) - \mathscr{L}_2(\tau) = \mathscr{L}_1(\tau)$.]

We refer to this null test as the *hysteresis test*. If, under the required conditions, the profiles are *not* equal, i.e. if there is a non-zero residual in their difference spectrum, then at least one of the assumptions of standard reverberation mapping is not valid.

The hysteresis test is based on identical $\mathscr{L}(\tau)$, and therefore non-linear line response cannot cause a non-zero residual. If such a residual *is* found, either MRD or the properties of the continuum source itself must be the cause.

In fact, to test the validity of the RM assumptions, it is not necessary that the continuum look-back light curves be identical for the two episodes. As we show below, there exist analogous null tests for the cases that the continuum look-back light curves are shifted [i.e $\mathscr{L}_2(\tau) = \mathscr{L}_1(\tau) + L_{\rm c}^0$] or scaled [i.e. $\mathscr{L}_2(\tau) = A\mathscr{L}_1(\tau)$].

Fig. 4 presents a schematic picture of these cases. In the light curve depicted there, episode II is identical to episode I plus a constant. If this constant were zero, the light curves for both episodes would be identical over a time $\tau_{\rm E}$. Therefore, if the assumptions of standard RM were fulfilled in the BLR, the observed line profiles would have to be identical at the end of these episodes if $\tau_{\rm E} > 2\tau_{\rm LT}$. Episode III is a scaled version of episode I. Tests based on the shifted and scaled episodes II and III will be discussed in the next two subsections.

5.1.2 *Differenced line profiles*

The hysteresis test can only be applied under special conditions. Therefore we seek a more generally applicable way to test standard RM, and to distentangle the problems outlined above. The goal is to eliminate pure reverberation effects, if possible, and to study the properties of the emission-line profile changes that are not due to reverberation.

'Differencing' is the most common way to study lines at different epochs in order to investigate line profile changes (e.g. Peterson 1987; Alloin, Boisson & Pelat 1988; Stirpe, de Bruyn & van Groningen 1989; Pérez et al. 1992). This method uses the direct difference between flux-calibrated profiles. It is usually unclear, however, whether the changes that are observed are *purely* due to reverberation effects or whether they represent real physical changes in the BLR, which renders it difficult to interpret the observed changes.

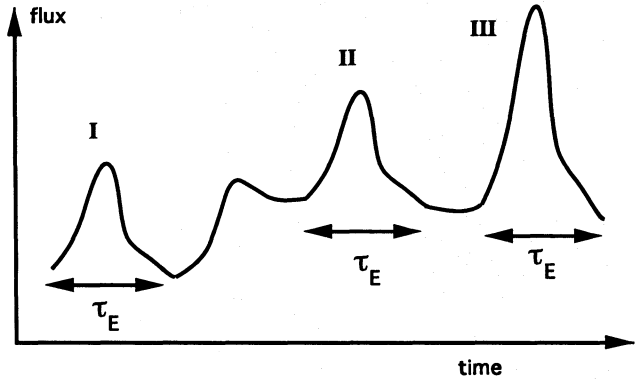

Figure 4. A schematic picture of the definition of the look-back light curve and the conditions to be met by the hysteresis test (see text).

The difference profile $L_{\rm d}(v, t_1, t_2)$ between profiles at epochs t_1 and t_2 is defined as

$$L_{\rm d}(v, t_1, t_2) \equiv L_\ell(v, t_2) - L_\ell(v, t_1), \tag{19}$$

which, under the standard assumption of RM that $\Psi_\ell(v, \tau)$ is time-invariant, becomes

$$L_{\rm d}(v, t_1, t_2) = \int {\rm d}\tau [\mathscr{L}_2(\tau) - \mathscr{L}_1(\tau)] \Psi_\ell(v, \tau), \tag{20}$$

where $\mathscr{L}(\tau)$ is the continuum look-back light curve as defined above. Note that $L_{\rm d}(v, t_1, t_2)$ is a function of v only, and that t_1 and t_2 are simply parameters defining the epochs of observations. Obviously, when the continuum look-back light curves of two episodes are simply shifted with respect to each other, i.e. $\mathscr{L}_2(\tau) = \mathscr{L}_1(\tau) + L_{\rm c}^{(1,2)}$, then

$$L_{\rm d}(v, t_1, t_2) = L_{\rm c}^{(1,2)} \int {\rm d}\tau \Psi_\ell(v, \tau) = L_{\rm c}^{(1,2)} \Phi_\ell(v), \tag{21}$$

where $\Phi_\ell(v)$ is the steady-state profile defined in Section 2.1. *It is thus possible to measure directly the steady-state profile from a variable source* – provided that we can find two instants in the light curve for which the condition $\mathscr{L}_2(\tau) = \mathscr{L}_1(\tau) + L_{\rm c}^0$ is fulfilled.

The assumptions of standard RM can now be tested by comparing two independent measurements of $\Phi_\ell(v)$. A null test of the RM assumptions thus requires at least three line profiles: $L_{\rm d}(v, t_1, t_2)$ must be compared either to a steady-state profile, or to a second-difference profile obtained from a third shifted-episode. $\Phi_\ell(v)$ can be eliminated either by dividing the two comparison profiles, which must then yield a result independent of v, or by normalizing the two profiles $[L_{\rm c}^0 \int {\rm d}v\, \Phi_\ell(v) = 1]$ and subtracting them:

$$\frac{L_{\rm d}(v, t_1, t_2)}{\int {\rm d}v\, L_{\rm d}(v, t_1, t_2)} - \frac{L_{\rm d}(v, t_3, t_4)}{\int {\rm d}v\, L_{\rm d}(v, t_3, t_4)} = \frac{L_{\rm c}^{(1,2)} \Phi_\ell(v)}{L_{\rm c}^{(1,2)} \int {\rm d}v\, \Phi_\ell(v)} - \frac{L_{\rm c}^{(3,4)} \Phi_\ell(v)}{L_{\rm c}^{(3,4)} \int {\rm d}v\, \Phi_\ell(v)} \equiv 0, \tag{22}$$

where t_4 might equal t_1 or t_2, or $L_{\rm d}(v, t_3, t_4)$ might equal an observed steady-state profile.

5.1.3 *Normalized line profiles*

Differencing profiles that are merely scaled versions of each other, i.e. that have the same *shape*, result in a difference profile that also is a scaled version of the input profiles. Therefore differencing of flux-calibrated profiles is not the best way to look for changes in the line shapes. If, however, before taking the difference, one normalizes the profiles to the same total flux, then two profiles with the same shape will result in a zero difference profile. Thus, normalization of emission-line profiles is a means of scaling away the total-line response and accentuating changes in the projected-velocity

distribution of the BLR clouds. The normalized emission-line profile (as defined in Section 3.1) now can be expressed in terms of the look-back time history, $\mathscr{L}(\tau)$, as

$$L_n(v,t)=\frac{\int \mathrm{d}\tau \mathscr{L}(\tau)\Psi_t(v,\tau)}{\int \mathrm{d}\tau \mathscr{L}(\tau)\Psi_t(\tau)}. \quad (23)$$

The difference between two normalized profiles can be written as

$$L_n(v,t_1)-L_n(v,t_2)=\frac{\int \mathrm{d}\tau \mathscr{L}_1(\tau)\Psi_t(v,\tau)\int \mathrm{d}\tau \mathscr{L}_2(\tau)\Psi_t(\tau)}{\int \mathrm{d}\tau \mathscr{L}_1(\tau)\Psi_t(\tau)\int \mathrm{d}\tau \mathscr{L}_2(\tau)\Psi_t(\tau)}$$
$$-\frac{\int \mathrm{d}\tau \mathscr{L}_2(\tau)\Psi_t(v,\tau)\int \mathrm{d}\tau \mathscr{L}_1(\tau)\Psi_t(\tau)}{\int \mathrm{d}\tau \mathscr{L}_1(\tau)\Psi_t(\tau)\int \mathrm{d}\tau \mathscr{L}_2(\tau)\Psi_t(\tau)}. \quad (24)$$

From equation (24) it is clear that if $\mathscr{L}_1(\tau)=A\mathscr{L}_2(\tau)$, i.e. if the continuum look-back light curves are scaled versions of each other, then $L_n(v,t_1)-L_n(v,t_2)\equiv 0$.

5.2 NGC 4151

We have searched for epochs with identical $\mathscr{L}(\tau)$ in the light curves of all objects for which we could locate published data spanning at least several look-back epochs, as inferred from their published lags. We discuss NGC 4151 here because three epochs with almost identical $\mathscr{L}(\tau)$ were found.

This object has been the subject of intensive study with the *IUE* satellite. A detailed discussion of all the *IUE* observations between 1978 and 1989 is given by Ulrich et al. (1991). An important conclusion of this paper is that the changes in the asymmetry of the C IV line are probably not caused by ionization differences alone, and that changes in the distribution of the fast-moving gas are required. Ulrich et al. do not, however, account for reverberation effects, i.e. the differences in the ionizing look-back light curve $\mathscr{L}$. In this section, we demonstrate that, using the same data, one can actually be more precise by applying the tests outlined in the previous section.

In the light curves published by Ulrich et al. (1991), there are three epochs at which nearly identical declines in the continuum flux are observed, namely 1983 October/November, 1985 May/June and 1988 November/December. Fig. 5 demonstrates this by plotting the three look-back light curves (see Section 5.1.1) of the continuum measured at 1715 Å. Note that the light curves are identical to within 20 per cent back to 15 d from $t=0$, and to within less than 10 per cent for 10 d from $t=0$. As discussed above, this time span $\tau_E=15$ d should be larger than twice the light traveltime in the C IV emitting region. Clavel (1990) showed that the peak of the cross-correlation function lies at 2 d for the bulk of the C IV line, and at 6 d for the core of the line. Hence the condition $\tau_E>2\times\tau_{LT}$ is fulfilled.

The profiles of the C IV λ1550 line as observed at these three epochs are reproduced in Fig. 6. Clearly, the three profiles are grossly different – the core is 25 per cent weaker in 1988 December than at the other two epochs, while large differences are also seen in the blue wing around 1545 Å. Similar differences in the core are observed in both C III λ1909 and He II λ1640. The variations around 1520 and 1570–1580 Å are probably due to real changes in the line wings in combination with changes in the intensities of the L_1, L_2 and L_2' satellite lines in C IV (see also Ulrich et al. 1991).

Non-linear line response can be excluded as the sole cause of these changes, because this test is unaffected by non-linearity. Note, however, that the possible occurrence of a non-linear line response is *not* excluded, as has been suggested in order to explain the response of the C IV line in NGC 5548 (Maoz 1992; Sparke 1993). We conclude that the only possible explanations for the observed differences in Fig. 6 are the following:

(i) mass redistribution occurs on a time-scale of several years;

(ii) the continuum is extended, or time-variable in its spectral or angular distribution over this time-span; or

(iii) the BLR is significantly larger than that deduced from the cross-correlation analysis for this object.

These results, taken together with those of NGC 3516, suggest that caution needs to be exercised when interpreting RM of the BLR.

5.3 Extension to evolutionary studies

The evolution of the TF – if it is found that standard RM is not applicable because the null tests have been violated – can be studied through consideration of the residuals. For

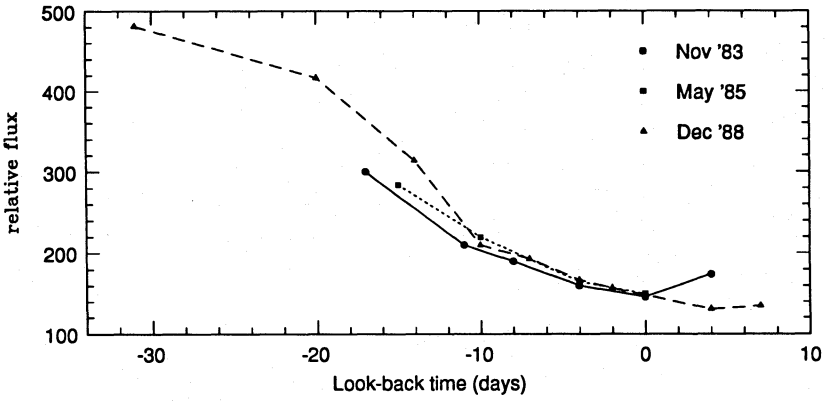

Figure 5. Three identical look-back light curves in the history of NGC 4151.

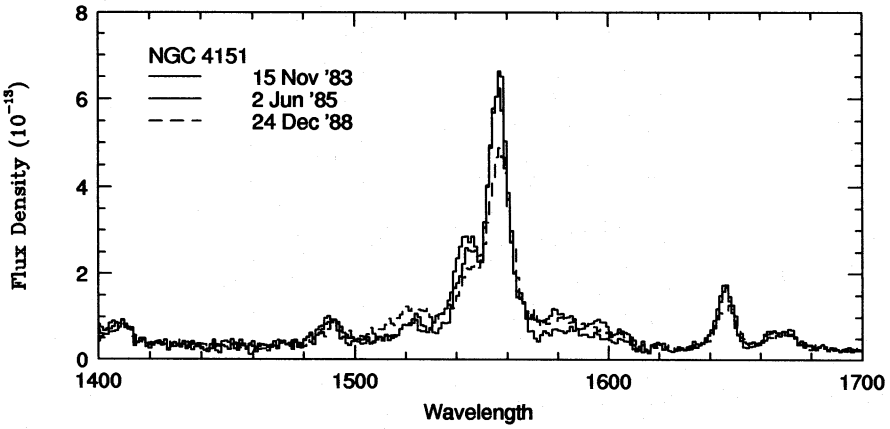

Figure 6. The three spectra of NGC 4151 belonging to the three instants with identical look-back light curves.

example, suppose that the condition of the hysteresis test *is* fulfilled by the continuum at two different epochs, but the test when applied to the line profiles gives a residual; then we *must* have

$$L_d(v, t_1, t_2) = \int d\tau \mathscr{L}(\tau)[\Psi_\ell(v, \tau; t_2) - \Psi_\ell(v, \tau; t_1)], \qquad (25)$$

where the term between square brackets is a measure of $(\partial/\partial t)\Psi_\ell(v, \tau; t)$, i.e. the time-dependence of the TF. Similarly, the method of differenced profiles can be extended to study the time-dependence of the steady-state profile $\Phi(v; t)$. The tests outlined in Section 5.1 are extremely powerful tools for the study of MRD, removing confusing reverberation effects.

5.4 Suggested monitoring strategies

Observing campaigns, for example, could be scheduled differently than they are currently, in order to test the assumptions of reverberation mapping and to study the evolution of the BLR. When one had accumulated a large data base of spectra and light curves one could stop monitoring spectroscopically and continue monitoring the continuum flux only. This could be done with a small telescope. Only if a certain repetition (identical, shifted or scaled) in the continuum light curve $[\mathscr{L}(\tau)]$ were observed would it be necessary to take a spectrum. In this way one could study the evolution of the BLR without pressing observing programme committees (OPCs) for enormous amounts of observing time on large telescopes. It *is* necessary initially to have a large data base of spectra [taken with different $\mathscr{L}(\tau)$], for which large telescopes and many observations are still needed. For certain objects like NGC 5548, however, a large data base already exists. It would also be necessary for OPCs to allow spectra to be taken at large telescopes at unpredictable times, i.e. as soon as a repetition in $\mathscr{L}(\tau)$ is found. A dedicated small telescope for continuum source monitoring of a number of AGN is also needed.

6 SUMMARY

In this paper we have examined the possible use of the wealth of detail contained in emission-line profiles, both to test the validity of the basic assumptions of reverberation mapping and to enhance the sensitivity to details in the velocity structure of the BLR and its evolution. We have defined a test – the hysteresis test – based on the truism that, if the basic assumptions of reverberation mapping are fulfilled, then *the observed line profiles must be identical at two different instants if the continuum light curves preceding these instants were identical over times corresponding to twice the light traveltime across the line-emitting region:* τ_{LT}. Here, τ_{LT} has been obtained from the observed lag under the assumption that reverberation mapping is valid. Most importantly, the hysteresis test is unaffected by non-linear line response.

If the test fails, it can do so only if (i) the BLR is larger than the size inferred from the observed lag, (ii) the continuum is extended, time-variable in its spectral or angular distribution, or (iii) mass redistribution occurs in the region on time-scales comparable to the length of the monitoring campaign. When applied to the *IUE* observations of NGC 4151, the one object for which appropriate data are currently available, the test fails. Whenever the test fails while its conditions are met, its result can be used to study the evolution of the BLR. We have proposed a new observing strategy to study the evolution of BLRs, provided that one has a large data base of spectra and light curves available, flexible OPCs at large observatories and a small dedicated telescope for continuum source monitoring.

Since few published continuum light curves contain multiple epochs over which the look-back light curves are identical, we have also considered methods to extract details about the structure of the BLR from the line profiles in such a way that possible violations of the basic assumptions are unlikely to remain hidden. We have re-expressed the standard transfer function used in reverberation mapping, dividing the transfer function into a dominant, steady-state part and a 'deviation' term (the 'Q'-function), and have shown that this 'deviation' term can be measured by evaluating normalized profiles. Such normalization, by removing the dominant effects of line intensity changes, enhances details in the velocity structure and its evolution. We have then applied this method to Balmer lines of NGC 3516, where time-dependent profile asymmetries are observed.

Since temporal changes in the line profiles appear to be present when they ought not to be, we now address the question of what could cause these observed differences.

Can the changes be due to continuum effects only? Were this the case, such effects would be expected to include one of the following.

(1) The observed continuum might not follow the ionizing continuum. Although the observations are not conclusive, however, several studies have shown a correlation between the optical/UV continuum and the ionizing continuum.

(2) The continuum source might radiate anisotropically, and this anisotropy might be temporally variable. It is highly unlikely, however, that this could happen on the time-scales observed here.

We thus think that the most likely explanation for the changes observed here is inhomogeneity of the BLR and MRD, or that the BLR is larger than we think, i.e. that the light curves do not go sufficiently far back in time. The results for NGC 3516 clearly indicate that this may be possible. The 25 per cent changes seen in the C IV profile of NGC 4151, however, are unlikely to be due solely to a large BLR; most of the BLR response lies at a distance from the continuum source, which is indicated by the peak of the TF and the CCF by the standard RM. Through the *Q*-concept, we have devised a new method for investigating the structure of the BLR, via normalized emission-line profiles, which is less biased to the region of highest response than the standard TF, and highly sensitive to changes in the emission-line profiles.

We thus conclude that direct observational evidence appears to suggest that broad-line regions are extended and have rather complicated velocity structures, or that changes occur in the matter distribution in the region on time-scales comparable to the variability time-scale. On longer time-scales, i.e. on the dynamical time-scale of the BLR, the observations of NGC 4151 suggest that matter redistributes itself within the BLR.

ACKNOWLEDGMENTS

JJP thanks the Astronomiska Observatoriet, Uppsala, for their hospitality and the Leverhulme Trust for financial support. We thank Enrique Pérez for a careful reading of the manuscript. This article is partly based on work carried out by the LAG (Lovers of Active Galaxies) collaboration. LAG is a consortium of mainly European astronomers which was established to study active galaxies using the International Time allocation at the Canary Islands' observatories, operated under the auspices of the Comité Científico Internacional.

REFERENCES

Alloin D., Boisson C., Pelat D., 1988, A&A, 200, 17
Andrillat Y., Souffrin S., 1968, Astrophys. Lett., 1, 111
Bahcall J. N., Kozlovsky B. Z., Salpeter E. E., 1972, ApJ, 171, 467
Blandford R. D., McKee C. F., 1982, ApJ, 255, 419 (BMK)
Cherepashchuk A. M., Lyutyi V. M., 1973, Astrophys. Lett., 13, 165
Clavel J., 1990, in Duschl W. J., Wagner S. J., Camenzind, eds, Variability of Active Galaxies. Springer-Verlag, Berlin, p. 31
Clavel J., 1991, in Miller H. R., Wiita P. J., eds, Variability of Active Galactic Nuclei. Cambridge Univ. Press, Cambridge, p. 343
Clavel J. et al., 1992, ApJ, 393, 113
Collin-Souffrin S., 1987, A&A, 179, 60
Collin-Souffrin S., Dumont S., Joly M., Tully J., 1986, A&A, 166, 27
Collin-Souffrin S., Dyson J. E., McDowell J. C., Perry J. J., 1988, MNRAS, 232, 539
Espey B., Carswell R. F., Bailey J. A., Smith M. G., Ward M. J., 1989, ApJ, 342, 666
Gaskell C. M., 1982, ApJ, 263, 79
Gaskell C. M., Sparke L. S., 1986, ApJ, 305, 175
Goad M. R., O'Brien P. T., Gondhalekar P. M., 1993, MNRAS, 263, 149
Horne K., Welsh W. F., Peterson B. M., 1991, ApJ, 367, L5
Krolik J. H., 1992, in Duschl W. J., Wagner S. J., eds, Physics of Active Galactic Nuclei. Springer-Verlag, Berlin, p. 173
Maoz D., 1992, in Duschl W. J., Wagner S. J., eds, Physics of Active Galactic Nuclei. Springer-Verlag, Berlin, p. 214
Maoz D. et al., 1991, ApJ, 367, 493
Maoz E., Smith P. S., Jannuzi B. T., Kaspi S., Netzer H., 1994, ApJ, 421, 34
Penston M. V., 1991, in Miller H. R., Wiita P. J., eds, Variability of Active Galactic Nuclei. Cambridge Univ. Press, Cambridge, p. 343
Pérez E., Robinson A., de la Fuente L., 1992, MNRAS, 255, 502
Perry J. J., 1993, in Sandqvist Aa., Ray T. P., eds, Central Activity in Galaxies – From Observational Data to Astrophysical Diagnostics. Springer-Verlag, Berlin, p. 25
Perry J. J., Dyson J. E., 1985, MNRAS, 246, 545
Peterson B. M., 1987, ApJ, 312, 79
Peterson B. M., 1988, PASP, 100, 18
Peterson B. M., 1993, PASP, 105, 247
Pounds K. A., Nandra K., Stewart G. C., 1992, in Duschl W. J., Wagner S. J., eds, Physics in Active Galactic Nuclei. Springer-Verlag, Berlin, p. 32
Robinson A., Pérez E., 1990, MNRAS, 244, 138
Skilling J., Bryan R. K., 1984, MNRAS, 211, 11
Sparks L. S., 1993, ApJ, 404, 570
Stirpe G. M., de Bruyn A. G., van Groningen E., 1989, A&A, 200, 9
Terlevich R., Tenorio-Tagle G., Franco J., Melnick J., 1992, MNRAS, 255, 713
Ulrich M.-H., Boksenberg A., Bromage G. E., Clavel J., Elvius A., Penston M. V., Perola G. C., Snijders M. A. J., 1991, ApJ, 382, 483
Wanders I., 1994, A&A, in press
Wanders I., Horne K., 1994, A&A, 289, 76
Wanders I. et al., 1993, A&A, 269, 39
Wills B. J., Netzer H., Wills D., 1985, ApJ, 288, 94
Yaqoob T., Warwick R. S., Makino F., Otani C., Sokoloski J. L., Bond I. A., Yamauchi M., 1993, MNRAS, 262, 435